Enzymatic Generation of the Chromopyrrolic Acid Scaffold of Rebeccamycin by the Tandem Action of RebO and RebD†

Annaleise R. Howard-Jones and Christopher T. Walsh*

Department of Biological Chemistry and Molecular Pharmacology, Harvard Medical School, Boston, Massachusetts 02115

Received August 25, 2005; Revised Manuscript Received October 3, 2005

ABSTRACT: During the biosynthesis of the fused six-ring indolocarbazole scaffolds of rebeccamycin and staurosporine, two molecules of L-tryptophan are processed to a pyrrole-containing five-ring intermediate known as chromopyrrolic acid. We report here the heterologous expression of RebO and RebD from the rebeccamycin biosynthetic pathway in *Escherichia coli*, and tandem action of these two enzymes to construct the dicarboxypyrrole ring of chromopyrrolic acid. Chromopyrrolic acid is oxidized by six electrons compared to the starting pair of L-tryptophan molecules. RebO is an L-tryptophan oxidase flavoprotein and RebD a heme protein dimer with both catalase and chromopyrrolic acid synthase activity. Both enzymes require dioxygen as a cosubstrate. RebD on its own is incompetent with L-tryptophan but will convert the imine of indole-3-pyruvate to chromopyrrolic acid. It displays a substrate preference for two molecules of indole-3-pyruvic acid imine, necessitating a net two-electron oxidation to give chromopyrrolic acid.

Rebeccamycin **1** and staurosporine **2** (Figure 1) are indolocarbazole antibiotics originally isolated from the actinomycetes *Lechevalieria aerocolonigenes* and *Streptomyces longisporoflavus*, respectively. Rebeccamycin is an inhibitor of DNA topoisomerase I, with a minimum inhibitory concentration of 1.75 μM (*1*). Staurosporine is one of the strongest inhibitors of protein kinases, displaying an IC_{50} of 2.7 nM for protein kinase C (*2*) and IC_{50}'s in the range of 1−20 nM for most protein kinases. Because of the importance of both the protein kinases and DNA topoisomerases in cell growth and proliferation, these two compounds have been extensively studied as antitumor drug candidates. Analogues of both rebeccamycin and staurosporine have entered clinical trials for the treatment of neoplastic tumors (*3*, *4*), renal cell cancer (*5*), and leukemia (*6*).

The fused six-ring indolocarbazole scaffold in **1** and **2** is representative of a variety of natural products and derived from the dimerization of two molecules of L-tryptophan (L-Trp)[1] via a complex set of oxidative transformations (*7*−*10*) (Scheme 1). Since this natural product scaffold is featured in molecules with an interesting range of biological activities, there has been substantial interest in understanding the enzymology of the oxidative dimerization and ring fusion

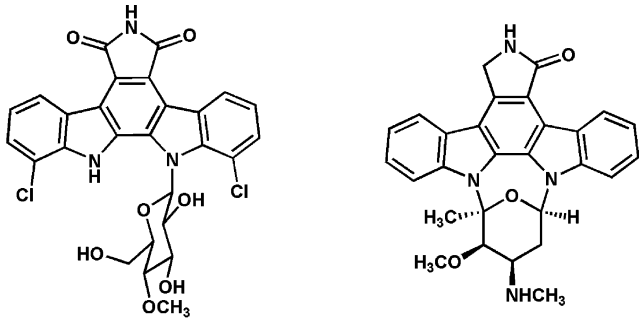

FIGURE 1: Chemical structures of rebeccamycin **1** and staurosporine **2**.

from the starting pair of L-Trp substrates. Subsequent N-glycosylation of the aglycone through the anomeric carbon of a glucose moiety (in the case of rebeccamycin) and through both C_1 and C_5 of L-ristosamine, the deoxyhexose sugar of staurosporine, followed by the action of methyltransferases (*11*), leads to the active natural products (Scheme 1). In the case of staurosporine, the enzymatic generation of the N−C linkage between one indole nitrogen and C5 of the aminodeoxyhexose is of notable interest as a novel transformation (*11*, *12*).

The biosynthetic gene clusters for rebeccamycin and staurosporine have been sequenced and functionally expressed in the heterologous host *Escherichia coli*, validating the minimal gene clusters and confirming the identity of key intermediates (*7*, *8*). However, little is known about the in vitro behavior, enzymology and mechanistic detail of many of the relevant biosynthetic enzymes.

Recent work within the Walsh group has established that RebF and RebH act as a two-component reductase/halogenase system (*13*). RebF is able to generate $FADH_2$, and RebH uses this reduced flavin, along with O_2 and chloride ion, to generate an oxidizing halogen equivalent.

† This work was supported by National Institutes of Health Grant GM020011.

* To whom correspondence should be addressed: Department of Biological Chemistry and Molecular Pharmacology, Harvard Medical School, 240 Longwood Ave., Boston, MA 02115. Telephone: (617) 432-1715. Fax: (617) 432-0438. E-mail: christopher_walsh@hms.harvard.edu.

[1] Abbreviations: 7Cl-IPA, 7-chloroindole-3-pyruvic acid; 7Cl-Trp, 7-chloro-L-tryptophan; CPA, chromopyrrolic acid; ES, electrospray mass spectrometry; FAD, flavin adenine dinucleotide; FMN, flavin mononucleotide; ICP-MS, inductively coupled plasma mass spectrometry; IPA, indole-3-pyruvic acid; IPTG, isopropyl β-D-thiogalactoside; LC−MS, liquid chromatography−mass spectrometry; MALDI-TOF, matrix-assisted laser desorption ionization time-of-flight; TFA, trifluoroacetic acid; tlc, thin-layer chromatography; L-Trp, L-tryptophan.

10.1021/bi051706e CCC: $30.25 © 2005 American Chemical Society
Published on Web 11/09/2005

Scheme 1: Overall Biosynthetic Route to Rebeccamycin (**1**) and Staurosporine (**2**), via CPA (**4**)[a]

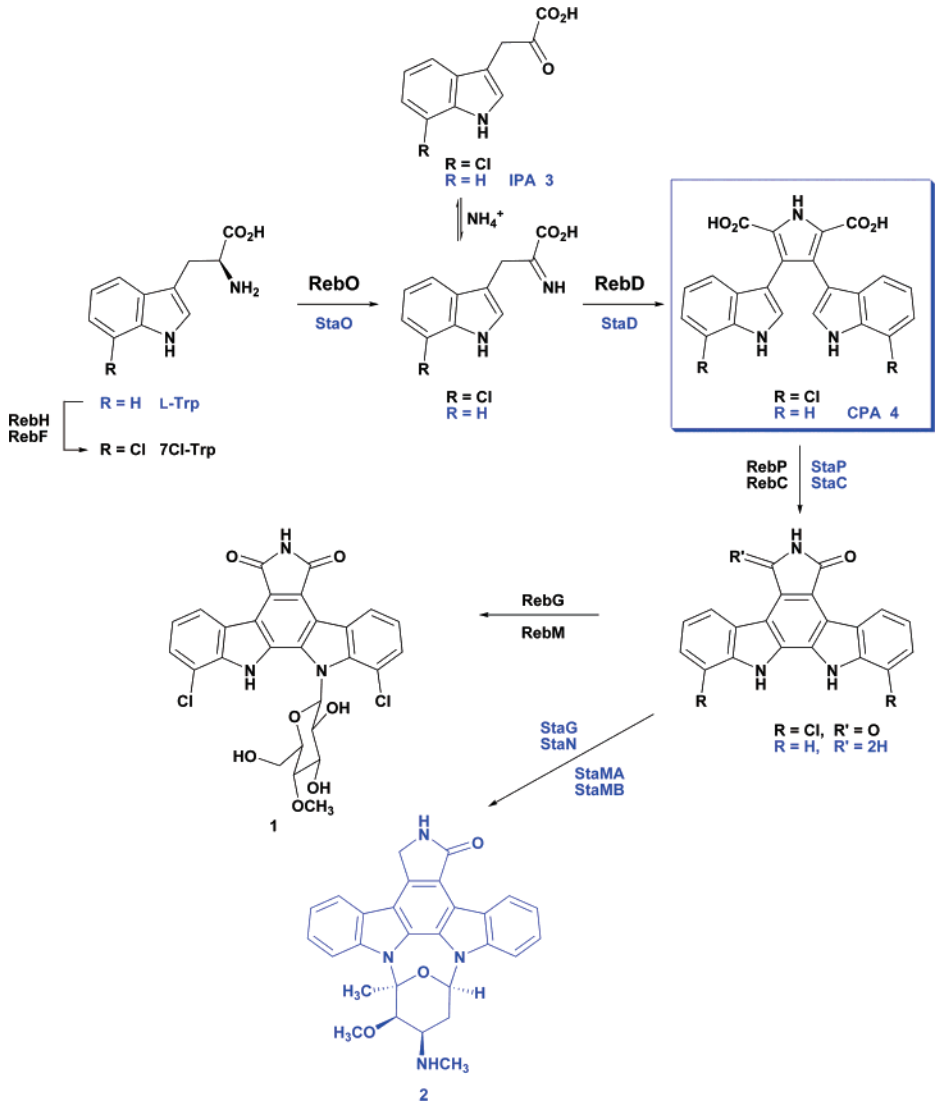

[a] Enzymes involved in the biosynthesis of rebeccamycin are colored black; those involved in the staurosporine biosynthetic pathway are colored blue.

This putative "Cl^+" equivalent is capable of reacting with L-Trp to yield 7-chloro-L-tryptophan (7Cl-Trp).

Inspection of the predicted functions of the *reb* (and homologous *sta*) genes has suggested that RebO is a flavoprotein, recently validated experimentally as an L-tryptophan oxidase (*14*), and that RebD, RebP and RebC function in subsequent biosynthetic steps (Scheme 1). Genetic studies indicate that RebD is required for formation of chromopyrrolic acid (CPA) **4** (*8*), and RebP and RebC are then responsible for the oxidative decarboxylation and ring fusion reactions that create the six-ring indolopyrrolocarbazole rebeccamycin aglycone (*8*). The transformation of compound **4** to the natural product **1** involves conversion of the dicarboxypyrrole ring to a maleimide moiety and represents unusual enzyme chemistry.

Herein, we describe the overproduction and purification of RebD from *E. coli* and reconstitution of CPA synthase activity, leading to construction of the dicarboxypyrrole ring of CPA (**4**) (Scheme 1). Catalytic activity was oxygen-dependent and most robust when RebO was used as the in situ generator of the imino form of indole 3-pyruvate (IPA) and when RebD was reconstituted with stoichiometric amounts of heme *b*. Two molecules of the IPA imine were shown to be the preferred substrates for RebD, requiring a net two-electron oxidation of the substrates during the RebD turnover cycle. RebD represents the first member in a novel subfamily of heme-containing oxidases, and shows some unusual oxygen consumption patterns. We propose a mechanism for the turnover of the IPA imine by RebD and for the overall formation of CPA (**4**) from L-Trp by the two-enzyme RebO/RebD system.

MATERIALS AND METHODS

Amino acids and $^{15}N_2$-labeled ammonium sulfate were purchased from Sigma-Aldrich; $^{15}N_2$-labeled L-Trp was obtained from Cambridge Isotope Laboratories. *E. coli* TOP10 and BL21(DE3) cells were obtained from Invitrogen. pET28a and pET22b plasmids were purchased from Novagen. Restriction enzymes were obtained from New England Biolabs. Nickel−nitrilotriacetic acid agarose (Ni−NTA) gel was obtained from QIAGEN. The HiLoad 26/60 Superdex 200 column was obtained from GE Healthcare. MALDI-TOF data were collected on an Applied Biosystems Voyager mass spectrometer. Electrospray mass spectra were collected

by liquid chromatography−mass spectrometry (LC−MS), using a Shimadzu LCMS-QP8000α instrument equipped with a Higgins Analytical (Mountain View, CA) Sprite Targa C18 column (20 mm × 2.1 mm) running at 0.8 mL/min (0 → 100% acetonitrile in water, with 0.1% formic acid) in positive ion mode. Analytical thin-layer chromatography (tlc) was performed using Merck precoated 60 F_{254} silica gel plates. NMR spectra were recorded on a Varian 500 MHz Fourier Transform NMR spectrometer. UV−visible spectra were collected on a Cary 50 Bio UV−visible spectrophotometer. DNA sequencing was performed by the Molecular Biology Core Facility (Dana-Farber Cancer Institute, Boston, MA).

DNA Isolation and Manipulation. L. aerocolonigenes ATCC 39243 was grown in yeast-malt extract medium (3 g/L yeast extract, 5 g/L malt extract, pH 7.0) for preparation of chromosomal genomic DNA. The culture was incubated at 26 °C and 250 rpm for 18 h prior to isolation of chromosomal DNA.

Standard methods for DNA isolation and manipulation were performed as described by Sambrook et al. (*15*). DNA fragments were isolated from agarose gels using a QIAGEN gel extraction kit.

Cloning, Expression, and Purification of RebO and RebD. Primers for *rebO* (5′-GGAGAG*CATATG*TCACGCGGACACAAG-3′ and 5′-GTC*AAGCTT*TCATCGTCCGTCGCCC-3′) and *rebD* (5′-GGAGAG*CATATG*AGCGTCTTCGACCTG-3′ and 5′-GTC*AAGCTT*TCGCGGTCCTTCCGTTGC-3′) contained *Nde*I and *Hin*dIII sites (italicized) and were used to amplify the relevant genes of interest. These orfs were cloned into the corresponding *Nde*I−*Hin*dIII sites of pET28a and pET22b, respectively. The correct sequences of the cloned expression vectors were confirmed by DNA sequencing.

E. coli BL21(DE3) cells overexpressing RebO were grown in Luria-Bertani medium supplemented with kanamycin (50 μg/mL). Cells were grown at 30 °C to an OD_{600} of 0.5, then induced at 15 °C with 100 μM isopropyl β-D-thiogalactoside (IPTG), and grown for a further 16 h at 15 °C. *E. coli* BL21(DE3) cells overexpressing RebD were grown in Luria-Bertani medium supplemented with ampicillin (100 μg/mL). Cells were grown at 15 °C to an OD_{600} of 0.5, then induced with 100 μM IPTG, and grown for a further 24 h at 15 °C.

Cells were harvested by centrifugation (20 min at 3000*g*) and resuspended in 20 mM Tris-HCl (pH 8.0), 300 mM NaCl, and 5 mM imidazole. Resuspended cells were lysed (two passes at 10000−15000 psi, Avestin EmulsiFlex-C5 high-pressure homogenizer), and the cell debris was removed by centrifugation (30 min at 15000*g*).

N-His_6-tagged RebO and C-His_6-tagged RebD were purified by Ni−NTA affinity chromatography. Eluted protein fractions were purified further by gel filtration chromatography using a HiLoad 26/60 Superdex 200 column. RebD was incubated with 10 equiv of hematin (heme *b*) at 4 °C for 1 h to achieve full heme reconsitution. Unbound heme was removed by gel filtration chromatography using the HiLoad 26/60 Superdex 200 column; fractions containing protein were collected and combined. The proteins were flash-frozen in liquid nitrogen and stored in 25 mM HEPES and 10% glycerol (pH 7.5) at −80 °C. Protein concentrations were determined using the method of Bradford, with bovine serum albumin (BSA) as a standard (*16*). The total yield of protein was 6 mg/L of culture for N-His_6-RebO and 8 mg/L of culture for C-His_6-RebD.

Biochemical Characterization of RebO. The molecular mass of RebO was determined using gel filtration by comparison to a set of known standards (Sigma-Aldrich). The nature and occupancy of the RebO cofactor were determined using analytical tlc and UV−visible spectrophotometry. Following denaturation (100 °C for 10 min) and precipitation of the protein, the supernatant was analyzed by tlc, with comparison to standard solutions of FAD and FMN. The flavin content of the solution was determined by UV-visible spectrophotometry, using the known extinction coefficient of FAD ($\epsilon_{450} = 11\,300\ M^{-1}\ cm^{-1}$).

Biochemical Characterization of RebD. The molecular mass of RebD was determined using gel filtration by comparison to a set of known standards (Sigma-Aldrich), and by MALDI-TOF mass spectrometry, using BSA as a standard. The heme content of RebD was analyzed using the pyridine hemochrome assay (*17*), and the iron content was determined using the Ferene S assay (*18*). Inductively coupled plasma mass spectrometry (ICP-MS) analysis was conducted by Elemental Research Inc. to detect the presence of seven metals in a sample of RebD (Fe, Mn, Co, Ni, Cu, Zn, and Mo); a standard solution containing only buffer was used to correct for any background presence of metals in the buffer solution.

Enzymatic Preparation of Chromopyrrolic Acid. E. coli BL21(DE3) cells overexpressing RebO and RebD (1 L of each culture) were grown and lysed as described above. To a solution of L-Trp (100 mg, 490 μmol) in 25 mM HEPES (pH 7.5, 250 mL) were added the crude cell extracts, and the mixture was incubated at 24 °C for 16 h. After the reaction had been quenched with trifluoroacetic acid (TFA, 250 μL), the mixture was lyophilized and filtered. Two rounds of reversed phase HPLC using a Beckman System Gold (Beckman Coulter) (0 → 100% acetonitrile in 0.1% TFA; Vydac C18 small pore column, 250 mm × 22 mm, 10 mL/min) afforded pure CPA (**4**), which displayed spectral properties consistent with those in the literature (*19*): *m*/*z* (ES^+) 386 ($[M + H]^+$, 100%), 368 ($[M - OH]^{\bullet+}$, 35%); UV−vis (25 μM in MeOH) $\epsilon_{220} = 42\,200\ M^{-1}\ cm^{-1}$, $\epsilon_{268} = 15\,400\ M^{-1}\ cm^{-1}$, $\epsilon_{325}(sh) = 2470\ M^{-1}\ cm^{-1}$; ^1H NMR (500 MHz, d_4-MeOH) δ 7.22 (dd, $J_{4,6} = 0.98$ Hz, $J_{4,5} = 8.3$ Hz, H_4), 7.15 (d, $J_{7,6} = 8.3$ Hz, H_7), 6.96 (ddd, $J_{4,6} = 0.98$ Hz, $J_{6,5} = 6.9$ Hz, $J_{6,7} = 8.3$ Hz, H_6), 6.86 (s, H_2), 6.79 (dd, $J_{5,6} = 7.3$ Hz, $J_{5,4} = 7.8$ Hz, H_5).

HPLC Activity Assays. Conversion of L-Trp to CPA was examined by analytical reversed phase HPLC, by mixing 1 mM L-Trp with RebD (from 10 nM to 1 μM) and RebO (from 0.3 to 6 μM), in the presence of BSA (0.1 mg/mL) in 75 mM HEPES buffer (pH 7.5). Reactions were quenched by addition of TFA (to a final concentration of 1%), and the protein was removed by centrifugation. HPLC assays were run on a Beckman System Gold (Beckman Coulter) with a Vydac C18 column (250 mm × 10 mm) at 1 mL/min using a gradient of 0 → 60% acetonitrile in 0.1% TFA. The elution profiles were monitored at 280 and 220 nm.

^{15}N Labeling Studies. ^{15}N-labeled substrates were used to probe the key substrate acceptance profile of RebD. Differentially labeled ammonium sulfate, IPA (**3**), and L-Trp were incubated with RebD with and without RebO under aerobic conditions to determine the origin of the nitrogens in CPA

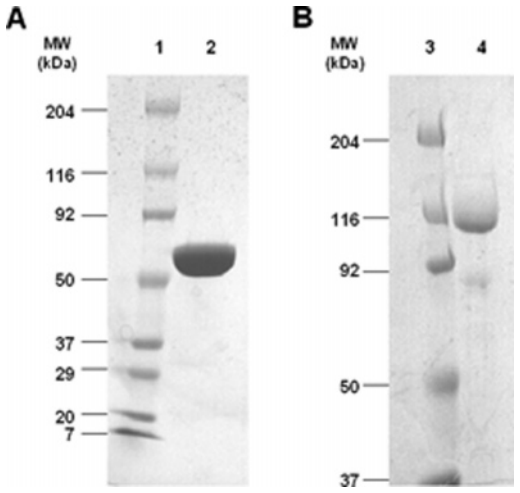

FIGURE 2: SDS−PAGE: lanes 1 and 3, molecular mass standards; lane 2, purified N-His_6-RebO; and lane 4, purified C-His_6-RebD.

and hence the key substrates for the enzyme. Following analysis by reversed phase HPLC, the CPA product was collected and analyzed by LC−MS in positive ion mode.

O_2 Electrode Assays. Oxygen consumption was assessed using a Hansatech D.W. oxygen electrode unit, based on a Clarke-type oxygen electrode (*20*). The instrument was calibrated by assessing the net oxygen consumption of 1.8 μM 2,3-dihydroxybiphenyl dioxygenase in the presence of 50, 100, and 150 μM 2,3-dihydroxybiphenyl (*21*). Oxygen consumption (RebO/RebD oxidase activity) and production (RebD catalase activity) rates were measured by reference to the calibration curve.

Anaerobic Experiments. Anaerobic assays were performed in a Unilab glovebox (Mbraun, Stratham, NH), with oxygen levels maintained at or below 2 ppm. All reagents and solutions were degassed by bubbling argon for 10 min prior to their introduction into the glovebox, and then equilibrated overnight to remove residual traces of oxygen. Preincubation of the reaction mixtures for 5 min with catalase (Sigma-Aldrich) (100 units/mL) was performed to convert hydrogen peroxide in solution to oxygen prior to introduction of RebD/RebO. Incubations were quenched immediately after removal from the glovebox by addition of 1% TFA.

RESULTS

Purification and Characterization of RebO and RebD. RebO was overproduced and purified as an N-terminal His_6-tagged protein with a molecular mass of 56 kDa (Figure 2A). Such L-amino acid oxidases frequently contain FAD cofactors, but FMN-dependent oxidases have also been observed (*22*). To determine the nature of the bound cofactor, analytical tlc of a solution derived by denaturation of a protein sample was conducted. This analysis revealed a spot that coeluted with an FAD standard, with no evidence of FMN in the solution (data not shown). UV−vis spectroscopic analysis confirmed the identity of the flavin as FAD (λ_{max} = 374 and 450 nm) and allowed for determination of the FAD occupancy at 70% (Figure 3).

RebD was overproduced and purified as a C-terminally His_6-tagged protein (Figure 2B), which ran as a dimer on a gel filtration column. Its molecular mass was determined to be 113 kDa by MALDI-TOF mass spectrometry. The iron content in the native protein (prior to heme reconstitution)

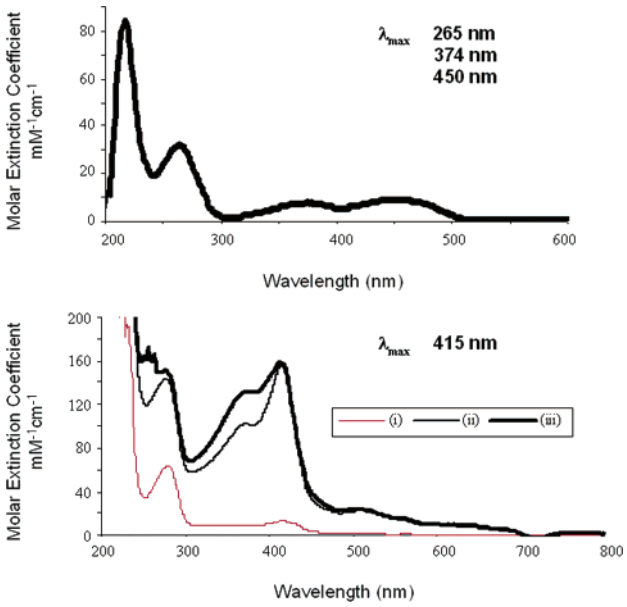

FIGURE 3: UV−visible spectrum of (A) a denatured N-His_6-RebO sample showing characteristic FAD features and (B) C-His_6-RebD (i) as purified, (ii) with 1.3 equiv of heme *b*, and (iii) with 1.8 equiv of heme *b*.

Table 1: Metal and Heme Content of RebD, As Determined by ICP-MS and Spectrophotometric Analysis, Respectively

	no. of metal centers/ polypeptide (ICP-MS)	no. of heme centers/ polypeptide (spectrophotometric analysis)
iron	2.92	1.8
zinc	0.17	
copper	0.06	
nickel	0.04	
manganese	0.002	
cobalt	–	
magnesium	–	

was found to be 1.1 equiv by the Ferene S spectrophotometric assay (*18*); the heme content was 0.1 equiv, as determined using the pyridine hemochrome UV−visible spectrophotometric assay (*17*). Heme reconsitution gave 1.2−1.8 equiv of heme per polypeptide. ICP-MS analysis of a sample containing 1.8 equiv of heme revealed the presence of 2.92 equiv of iron (Table 1). Thus, it is apparent that, in addition to the heme content, RebD also contains 1 equiv of non-heme iron. The enzyme has been shown to contain no inorganic sulfide, as determined by a methylene blue-dependent spectrophotometric assay for S^{2-} (data not shown) (*23*, *24*). This result eliminates the possibility that the non-heme iron of RebD forms part of an iron−sulfur cluster.

Chromopyrrolic Acid Synthase Activity of RebD and the Increase in Activity in Tandem Incubations of RebO and RebD. On the basis of previous in vivo studies (*8*), RebD was proposed to catalyze the formation of CPA (**4**) from IPA (**3**) during rebeccamycin biosynthesis. We were interested in determining the activity of RebD in forming CPA (**4**), and in ascertaining the substrate requirements of this enzyme. Because of the limited availability of 7Cl-Trp, the natural substrate for the RebO/RebD system (*14*), much of this study on the tandem action of RebO and RebD was performed using L-Trp as the substrate.

The turnover of L-Trp and IPA (**3**) by RebD was investigated, and evidence of CPA formation was verified

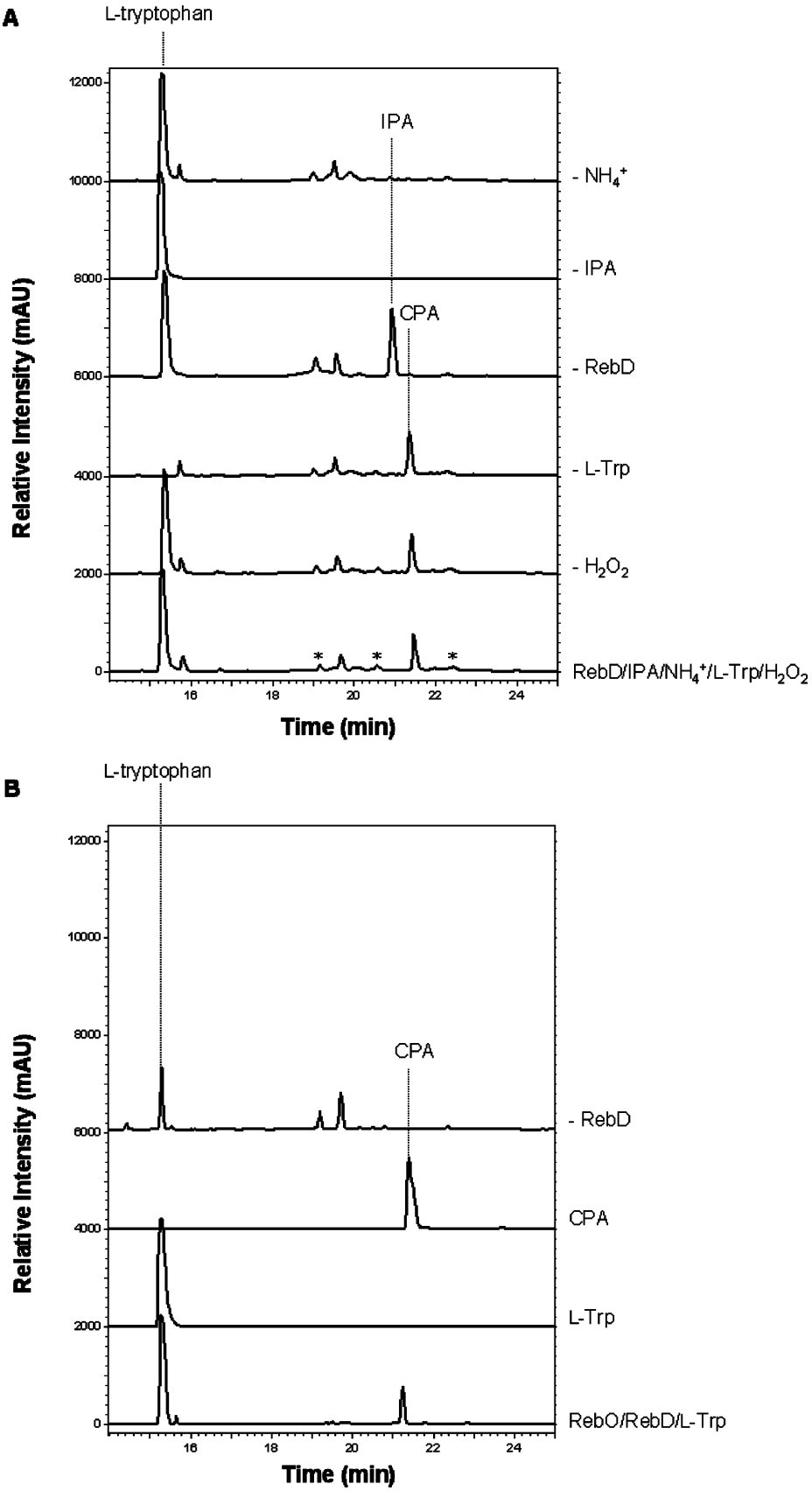

FIGURE 4: HPLC traces (280 nm) showing formation of CPA by RebD and RebO/RebD-mediated turnover. (A) RebD-mediated turnover of 1 mM IPA (**3**) and 10 mM $(NH_4)_2SO_4$ in the presence of 0.1 mg/mL BSA, 1 mM L-Trp, 10 μM H_2O_2, and 1 μM RebD in 75 mM HEPES (pH 7.5). (B) RebO/RebD-mediated turnover of 1 mM L-Trp in the presence of 0.1 mg/mL BSA by 3 μM RebO and 1 μM RebD in 75 mM HEPES (pH 7.5). Reactions were quenched after incubation for 18 h at room temperature. Oxidative degradation products are indicated with asterisks.

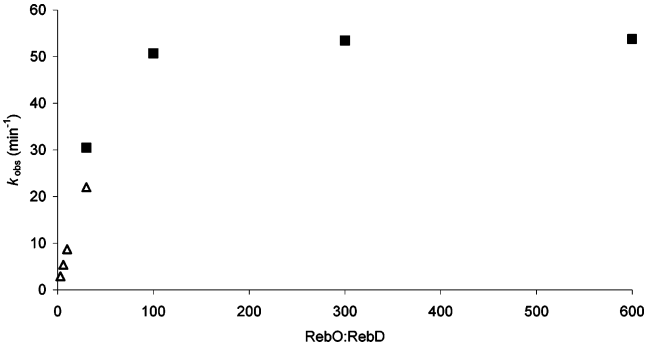

FIGURE 5: k_{obs} for CPA production by RebD [100 (△) or 10 nM (■)] and RebO (0.3−6 μM) in the presence of 1 mM L-Trp, 0.1 mg/mL BSA, and 75 mM HEPES (pH 7.5).

by analytical HPLC, UV−visible, and mass spectrometric analysis, by comparison to an authentic sample generated in this work. Heme-reconstituted RebD catalyzes the formation of CPA (**4**) from IPA (**3**) and ammonium ion; L-Trp is not required. Under these conditions, however, turnover is slow ($k_{obs} = 2$ min^{-1}) and extensive oxidative degradation of IPA (**3**) is observed (Figure 4A; oxidative degradation products indicated with asterisks). Prior to reconsitution with heme, incubation of the naturally isolated enzyme under the same conditions gives no appreciable CPA formation over a period of 24 h (data not shown). All reconstituted samples of RebD with a heme content of ≥1 equiv displayed the same activity profiles. This suggests that a single heme center is intimately involved in the catalytic process.

The turnover of L-Trp by a two-component RebO/RebD system gives markedly improved efficiency and catalytic rates with minimal off-pathway oxidative degradation. This activity requires the presence of L-Trp, RebO, RebD, and dioxygen (Figure 4B), but no additional cofactors are necessary.

Since the physiologically relevant activity of RebD appears to be that observed in the presence of RebO, most assays were conducted using the two enzymes in tandem. To further probe the activity of RebD, the RebO:RebD ratio was altered to determine the ratio at which CPA formation was not dependent on the concentration of RebO (Figure 5). It was hence possible to use sufficient RebO (≥300:1) such that this was not the limiting component, and the rate of formation of CPA (**4**) was linear with RebD concentration, following an initial lag. Under these conditions, the turnover rate for RebD (in the presence of RebO) in the linear time period was 53 min^{-1}, a 26-fold increase in rate over that with the IPA imine and RebD alone.

Under the same conditions, the RebO/RebD system was able to turn over 7Cl-Trp with a k_{obs} of 32 min^{-1}. The relative difference in observed rates for 7Cl-Trp versus its deschloro analogue is curious given the observed in vivo formation of rebeccamycin (which has two chlorines) by the Reb system. However, it is possible that the greater catalytic efficiency of RebO for 7Cl-Trp versus L-Trp (*14*), coupled with the apparent rapid uptake of the 7-chloroindole-3-pyruvic acid (7Cl-IPA) imine (or IPA imine) product by RebD, may provide the observed preference for formation of the dichloro-CPA product in vivo.

At high RebO:RebD ratios (approximately ≥5:1), there was extensive buildup of IPA (**3**) in solution. To facilitate more ready analysis of CPA formation and to minimize off-pathway oxidation, most of our turnover assays were conducted at a 3:1 RebO:RebD ratio. At this ratio, the intermediate IPA imine was effectively shuttled through to CPA with minimal apparent buildup of IPA.

The possibility that RebD is acting as a nonspecific peroxidase was investigated by conducting a control experiment involving co-incubation of horseradish peroxidase with L-Trp and RebO. This incubation mixture showed no evidence of CPA formation after 24 h (data not shown), suggesting that RebD is not functioning simply as a generic peroxidase.

Identification of Key Substrates for RebD. Given that maximal CPA formation was observed in the presence of both RebO and RebD, assays were generally conducted using the tandem enzyme system with L-Trp as the initial substrate. Therefore, a key issue to be addressed was the identification of the actual substrates for RebD. In particular, the preference of the enzyme for turning over either two IPA-like molecules or one IPA (**3**) and one L-Trp was of interest. These two alternative substrate preferences are associated with different oxidative requirements; the former transformation requires a two-electron oxidation, while the latter requires the removal of four electrons. An understanding of the substrate requirements of RebD would thus provide evidence for the role of RebD in performing either a two-electron or a four-electron substrate oxidation. To shed light on this issue, experiments using differential isotopic labeling were employed to determine the origin of the nitrogens of CPA (**4**) and, by extension, the different sections of the CPA molecule.

The RebO/RebD-mediated turnover of L-Trp gives the CPA product with *m*/*z* 386, corresponding to the $[M + H]^+$ molecular ion peak (Figure 6A). Incubation of RebO and RebD (3:1 ratio) with 1 mM ($^{15}N_2$)-L-Trp, 1 mM (^{14}N)IPA, and 10 mM ($^{14}N_2$)ammonium sulfate resulted in a CPA product with *m*/*z* 386 (Figure 6B), corresponding to the molecular ion containing three ^{14}N isotopes. This result suggests that neither the nitrogen of the indole ring nor that of the α-amino group of L-Trp is incorporated into the final CPA product (**4**). The turnover of 1 mM ($^{14}N_2$)-L-Trp, 1 mM (^{14}N)IPA, and 10 mM ($^{15}N_2$)ammonium sulfate gives an *m*/*z* 387 molecular ion peak for CPA (Figure 6C), presumably incorporating the ammonium nitrogen in the dicarboxypyrrole ring. Hence, with a 1:1 L-Trp:IPA ratio, RebD does not incorporate L-Trp directly into the product CPA, but accepts two IPA-derived substrates and incorporates 1 equiv of ammonium ion. In the absence of RebO, an analogous product distribution is observed. RebD converts 1 mM ($^{15}N_2$)-L-Trp, 1 mM (^{14}N)IPA, and 10 mM ($^{14}N_2$)ammonium sulfate to an *m*/*z* 386 peak; 1 mM ($^{14}N_2$)-L-Trp, 1 mM (^{14}N)IPA, and 10 mM ($^{15}N_2$)ammonium sulfate result in an *m*/*z* 387 peak (data not shown).

Given the preference of RebD to accept IPA (**3**) as a substrate over L-Trp in a 1:1 mixture (in the presence of ammonium ion), the predominant pathway appears to be via two IPA-like reaction partners, and hence must involve a two-electron substrate oxidation. Therefore, a four-electron oxidation of one L-Trp and one IPA by RebD is not the major biological pathway.

When the L-Trp:IPA ratio is altered to 10:1 [1 mM ($^{15}N_2$)-L-Trp, 0.1 mM (^{14}N)IPA, and 10 mM ($^{14}N_2$)ammonium sulfate], the CPA that is produced has two major peaks in the mass spectrum at *m*/*z* 388 (corresponding to the

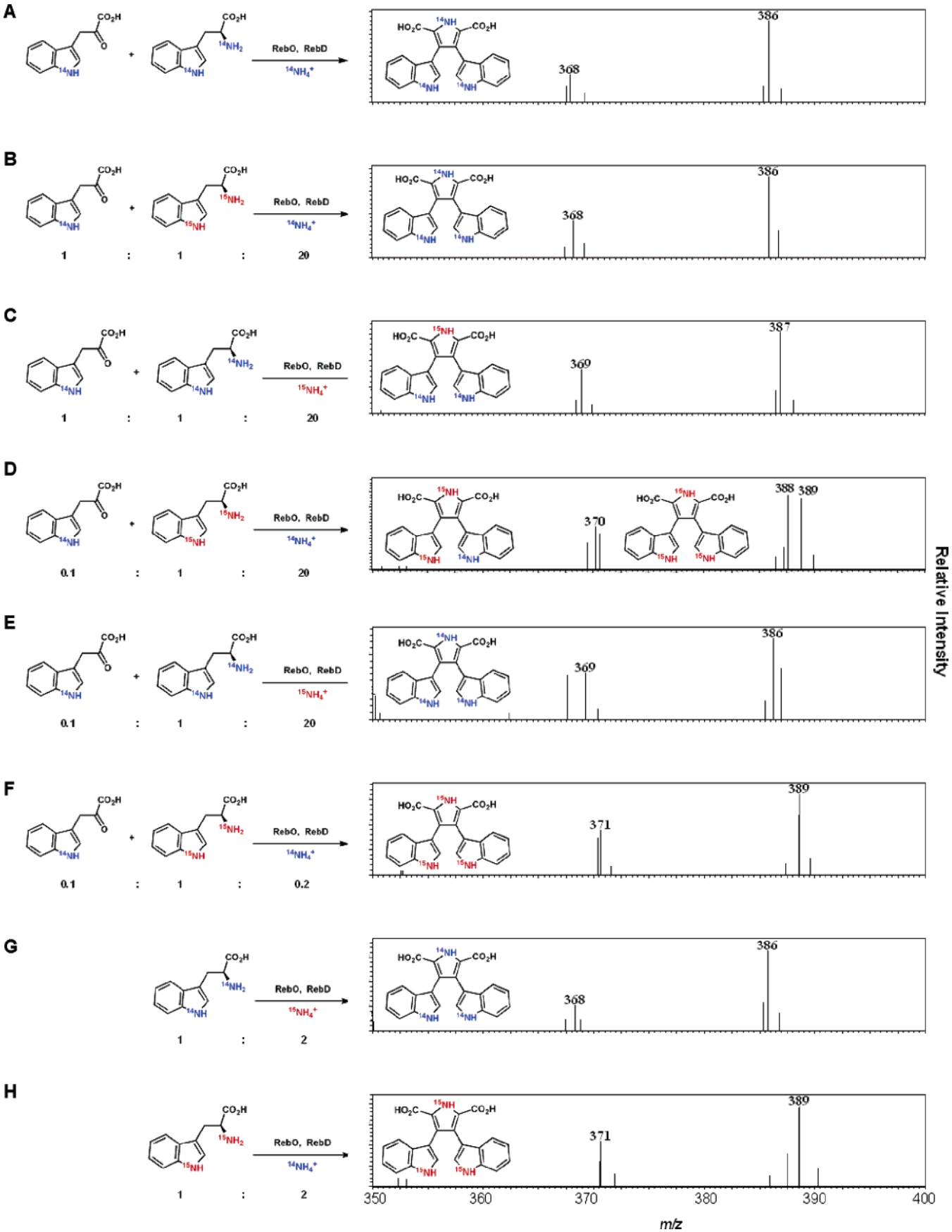

FIGURE 6: Mass spectrum of the CPA product derived from reaction of differentially labeled L-Trp, ammonium sulfate, and IPA (**3**). Following reaction of RebD (with or without RebO) with L-Trp, IPA (**3**), and/or ammonium sulfate for 21 h at room temperature, reactions were quenched by addition of 1% TFA and centrifugation. The resulting supernatant was analyzed by reversed phase HPLC and the CPA peak ($R_t \sim 24$ min) collected and studied by LC−MS (positive ion mode). ^{14}N labels are depicted in blue and ^{15}N labels in red. The ion at *m*/*z* 386 corresponds to the $[M + H]^+$ molecular ion peak, and that at *m*/*z* 368 corresponds to the $[M - OH]^{\bullet+}$ fragment ion of $(^{14}N_3)$CPA.

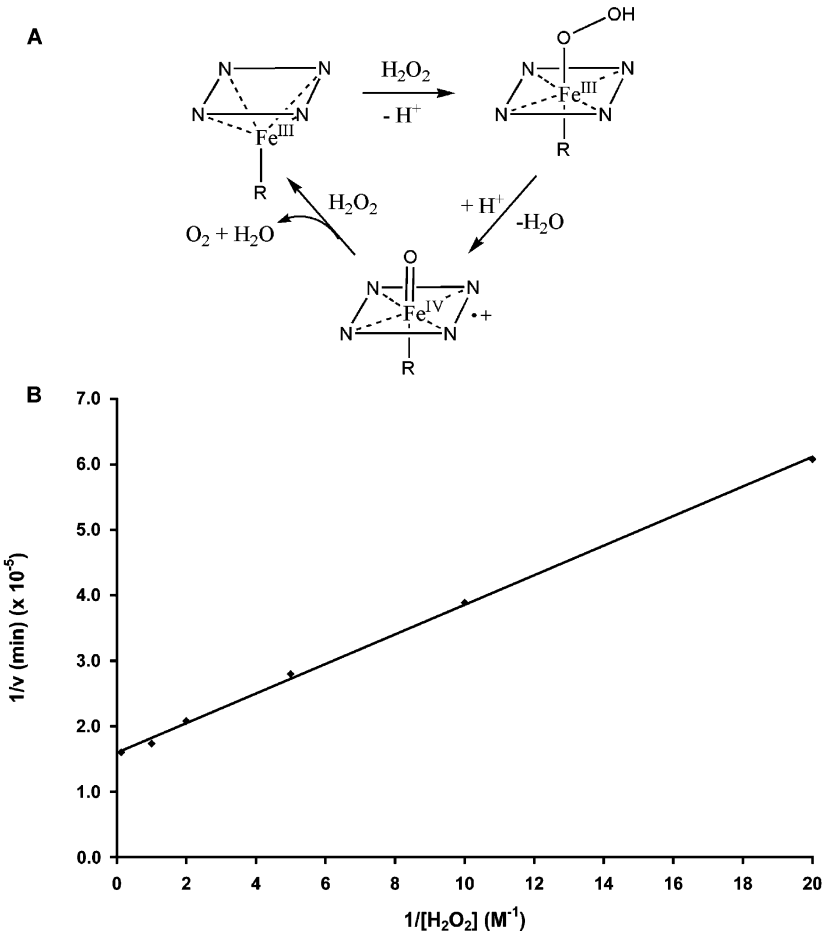

FIGURE 7: (A) Proposed mechanism for catalase activity of RebD and (B) double-reciprocal plot of velocity vs hydrogen peroxide concentration. Hydrogen peroxide (from 50 mM to 8 M) was incubated with 50 nM RebD and 75 mM HEPES (pH 7.5), and initial rates were determined using an oxygen electrode system.

incorporation of two ^{15}N labels) and *m*/*z* 389 (corresponding to a product bearing three ^{15}N labels) (Figure 6D). The *m*/*z* 388 peak may arise from a compound containing either ^{15}N labels in the two indole rings or ^{15}N labels in one of the indoles and in the dicarboxypyrrole ring. To clarify which of these is the most likely product, the isotopic pattern in the substrates was rearranged and the mass spectrum of the CPA product was again recorded. Incubation of 1 mM ($^{14}N_2$)-L-Trp, 0.1 mM (^{14}N)IPA, and 10 mM ($^{15}N_2$)ammonium sulfate gave the major peak for CPA in the mass spectrum at *m*/*z* 386 (Figure 6E), indicating that nitrogen from ammonium is not incorporated into the CPA product at this substrate ratio. Therefore, the dicarboxypyrrole nitrogen is primarily derived from the L-Trp moiety, presumably via the imine product of RebO turnover. The second indole ring must therefore be derived from a free molecule of IPA (**3**) or its imine.

If the concentration of ammonium ion is reduced 100-fold, the isotope distribution of the product is again altered. Incubation of the RebO/RebD system with 1 mM ($^{15}N_2$)-L-Trp, 0.1 mM (^{14}N)IPA, and 0.1 mM ($^{14}N_2$)ammonium sulfate gives a single major peak at *m*/*z* 389, with no evidence of an *m*/*z* 388 product (Figure 6F). This presumably arises due to the condensation of two IPA imine molecules directly furnished by RebO-mediated L-Trp oxidation, with no incorporation of free IPA.

The ammonium ion concentration is intimately linked to the IPA ketone−IPA imine equilibrium (indicated in Scheme 1). Hence, a 100-fold decrease in the amount of ammonium would result in a drastic shift in the equilibrium position toward the IPA ketone form and away from the imine. The fact that this also dramatically alters the source of the CPA nitrogen atoms suggests that the second half of the CPA product is also derived from an IPA imine. This result is thus consistent with the hypothesis that the actual substrates for RebD are two molecules of the IPA imine.

The incubation of the RebO/RebD system with L-Trp and ammonium sulfate, in the absence of IPA (**3**), was carried out to further assess the extent of hydrolysis and amine exchange of the putative IPA imine product of RebO turnover. Thus, incubation of the RebO/RebD system with 1 mM ($^{14}N_2$)-L-Trp and 1 mM ($^{15}N_2$)ammonium sulfate (Figure 6G) or 1 mM ($^{15}N_2$)-L-Trp and 1 mM ($^{14}N_2$)ammonium sulfate (Figure 6H) (in the absence of IPA) gives exclusively the product bearing the isotope distribution pattern of the L-Trp. It therefore seems that no significant hydrolysis and exchange of the nitrogen of the putative imine intermediate are observed during RebO/RebD-mediated CPA formation.

Characterization of RebD as a Heme Protein with Catalase Activity. RebD acts as an efficient catalase, effecting the disproportionation of hydrogen peroxide to give oxygen and (presumably) water. Heme reconstitution is required for maximal catalase activity, which is presumed to follow a typical heme catalase mechanism (Figure 7A). The double-reciprocal plot of initial velocity versus hydrogen peroxide concentration gives a linear trace (Figure 7B). This catalase

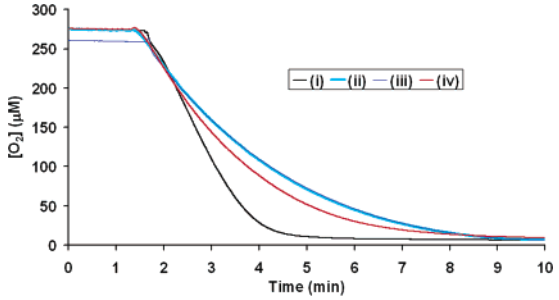

FIGURE 8: Oxygen consumption time course for turnover of 10 mM L-Trp in 0.1 mg/mL BSA and 75 mM HEPES (pH 7.5) by (i) RebO (3 μM), (ii) RebO (3 μM) and RebD (1 μM), (iii) RebO (3 μM), RebD (1 μM), and catalase (100 units/mL), and (iv) RebO (3 μM) and catalase (100 units/mL).

activity of RebD is characterized by a k_{cat} of 64 000 ± 1000 min^{-1} and a K_m of 150 ± 10 mM (a somewhat high value for a catalase, which would typically have a K_m around 25 mM).

Consistent with this observation is the fact that the RebO/RebD-mediated formation of CPA from L-Trp does not result in net production of hydrogen peroxide. The RebD catalase activity is presumably responsible for the disproportionation of any RebO-derived hydrogen peroxide produced. The catalase activity of RebD is reduced in the presence of IPA (**3**) (data not shown), which may indicate the involvement of a single active site in both CPA production and H_2O_2 disproportionation.

Oxygen Consumption Studies on RebO/RebD. The rate of oxygen consumption during turnover of L-Trp by RebO and by the RebO/RebD system was investigated. In the presence of catalase, the RebO oxygen consumption rate was reduced by 1.7-fold (Figure 8), consistent with the regeneration of 0.5 equiv of dioxygen by hydrogen peroxide disproportionation. In the presence of RebD, the oxygen consumption rate was reduced by 2.1-fold relative to that in the presence of RebO alone. This result is inconsistent with a noninteractive two-enzyme system, which would require a reduction of less than 1.7-fold, due to the RebD catalase activity (giving a 1.7-fold reduction) and additional oxygen consumption by RebD-mediated turnover. It therefore seems that RebO and RebD are mutually influenced by one another, resulting in a reduction in the overall oxygen consumption rate. Addition of catalase to the RebO/RebD system has no significant effect on the rate of oxygen consumption or on the final CPA concentration (data not shown).

Anaerobic Studies on RebD Turnover. To identify the co-oxidant involved in RebD-mediated CPA formation, the turnover of IPA (**3**) by RebD under anaerobic conditions, in the presence and absence of RebO, was examined (Figure 9). This experiment was performed both with and without hydrogen peroxide to test for possible peroxidase activity. In the absence of both dioxygen and hydrogen peroxide, CPA (**4**) was not formed by either RebD in isolation or the RebO/RebD system. In the presence of hydrogen peroxide and the absence of dioxygen, CPA (**4**) was formed, along with a range of oxidation shunt products.

The observed CPA formation under these conditions may be indicative of a peroxidase activity or may simply be due to RebD acting as a catalase to generate dioxygen, allowing for an oxidase-type turnover. Therefore, it was important to parse the catalase activity of RebD from a possible peroxidase activity. Thus, the aforementioned experiment was repeated, but the reaction mixtures were preincubated with catalase prior to the introduction of RebD (with or without RebO). Such a preincubation with catalase would ensure the complete conversion of the hydrogen peroxide in solution to dioxygen prior to any RebD-mediated turnover. Under these conditions, CPA (**4**) was indeed formed. The presence of catalase had little effect on the conversion of IPA (**3**) to CPA (**4**) by RebD or by the RebO/RebD system (Figure 9).

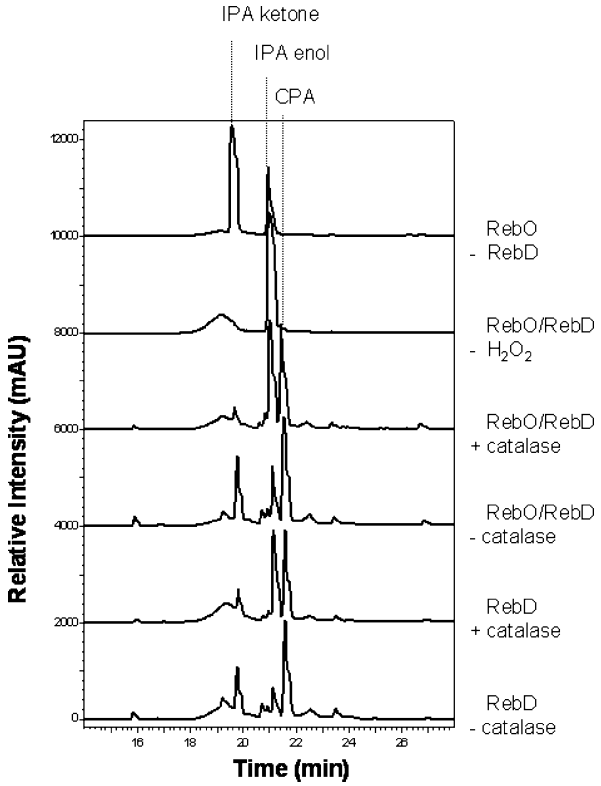

FIGURE 9: HPLC traces (280 nm) of products formed by anaerobic turnover of 1 mM IPA (**3**) and 10 mM $(NH_4)_2SO_4$ by 1 μM RebD (with and without 3 μM RebO) in 0.1 mg/mL BSA and 75 mM HEPES (pH 7.5) in the presence of 1 mM hydrogen peroxide, with and without a catalase (100 units/mL) preincubation step.

DISCUSSION

The conversion of two molecules of the primary metabolite L-Trp to the six-ring bisindolopyrrolocarbazole scaffold of the rebeccamycin aglycone is a remarkably short and efficient biological oxidation process, involving only four gene products (RebO, RebD, RebP, and RebC). It has recently been established that RebO is a flavin-dependent L-tryptophan oxidase, akin to the well-known L-amino acid oxidases, generating the imine form of indole 3-pyruvate, with concomitant two-electron reduction of O_2 to H_2O_2 (*14*). 7Cl-Trp is the preferred substrate for RebO (*14*), which generates the imine form of 7Cl-IPA as its immediate oxidation product.

RebD, an intriguing member of the rebeccamycin biosynthetic system, has very few homologues. Homology analysis of the RebD amino acid sequence reveals a 54% level of identity with StaD, the analogous enzyme from the staurosporine biosynthetic cluster (*9*, *10*), and a 34% level of identity with VioB, an enzyme involved in a related transformation during the biosynthesis of the antibacterial pigment violacein (*25*, *26*). As with RebD, neither of these

homologues has been overproduced, purified, or characterized in vitro. This study on RebD therefore represents a significant advance in our understanding of this subfamily of proteins and, by extension, the broader field of heme proteins.

Once we had heterologously expressed and purified RebD in soluble form, we observed the red color characteristic of the heme prosthetic group in the purified C-His_6-tagged protein. The heme content was substoichiometric but could be brought back to stoichiometric and suprastoichiometric levels after heme addition and gel filtration. It is interesting to note that, while RebD overproduced as a heme-containing protein, its amino acid sequence displays no apparent signature motifs for heme binding domains, cytochrome P450s, or commonly encountered heme-dependent oxidases. Given that a construct expressing only RebO and RebD in *Streptomyces albus* yields CPA (**4**) (*8*), the presence of bound heme is in accord with the expectation that RebD might be a redox enzyme.

When IPA (**3**) and ammonium ions were incubated with purified RebD, a slow but significant rate of CPA (**4**) formation was detected. This reaction was dependent on dioxygen, consistent with the expectation that RebD is functioning as a heme-protein oxidase to catalyze the oxidative dimerization of two L-tryptophan-derived molecules to CPA.

On the other hand, tandem incubations of RebO and RebD gave robust formation of CPA (**4**). It is tempting to suggest that the acceleration of RebD activity in the presence of RebO arises from a RebO−RebD complex in which RebD displays enhanced catalytic efficiency. However, we do not see evidence of a stable heteromeric RebO−RebD complex by surface plasmon resonance (K. Phillips, personal communication) or by analytical gel filtration (data not shown).

Tandem RebO−RebD activity is presumably favored by Nature due to the inherent instability of the putative intermediate, IPA imine. The imine is readily hydrolyzed in solution, existing in equilibrium with the predominant ketone form, IPA (**3**) (and its enol tautomer) (Scheme 1). More importantly, however, IPA (**3**) is very unstable and rapidly degrades in solution to give a range of oxidative byproducts. Therefore, the concerted functioning of the RebO/RebD system appears to prevent the buildup of significant amounts of IPA (**3**) and its imine in solution, effectively shepherding the imine further down the biosynthetic chain (Scheme 1). The product of RebO/RebD turnover, CPA (**4**), is significantly more stable and is not observed to degrade in buffered solutions (pH 7.5) at room temperature over a period of 7 days.

When RebD is added to solutions of RebO and L-Trp, the overall O_2 consumption rate is reduced. At first, this result seemed anomalous, given our prior observations that the RebD-mediated formation of CPA (**4**) from the IPA imine is dependent on O_2. Hence, we expected that addition of RebD would give an increase in the O_2 consumption rate. However, this discovery led to the finding that RebD displays robust and efficient catalase activity (in the absence of the substrates required for CPA synthase activity) to generate dioxygen in solution. Since RebO generates peroxide as a coproduct along with the IPA imine, the addition of RebD allows disproportionative scavenging of H_2O_2 and a net reduction in the rate of oxygen consumption.

The results described herein outline the oxidative biosynthetic pathway leading from L-Trp to CPA (**4**), via the tandem action of RebO and RebD. These two enzymes are able to catalyze the formation of this five-ring pyrroledicarboxylate-containing intermediate of rebeccamycin through formation of the IPA imine and subsequent oxidative coupling. On the basis of extensive ^{15}N labeling studies, the favored substrates for RebD appear to be two molecules of IPA imine. This imine is the immediate product of the turnover of L-Trp by RebO (Scheme 1). The predominant reaction pathway for RebD-mediated turnover is therefore an overall two-electron oxidation of the IPA imine substrates, resulting in formation of CPA.

Due to the efficient catalase activity of RebD, distinguishing between oxygen and hydrogen peroxide as the preferred co-oxidant in CPA formation is not a trivial undertaking. It is clear, however, that RebD is competent in accepting dioxygen as a cosubstrate in the oxidative coupling of two IPA imines to give CPA; hydrogen peroxide is not required. Under anaerobic conditions, however, the presence of hydrogen peroxide allows for the formation of CPA. Preincubation with catalase (to disproportionate all of the hydrogen peroxide to oxygen) gives no change in the overall product distribution (Figure 9), leading weight to the argument that H_2O_2 is converted to dioxygen in situ, via the catalase activity of RebD. Furthermore, the net oxygen consumption rate of the RebO/RebD system is not altered by the presence of catalase (Figure 8, ii and iii).

It therefore seems most likely that RebD is an oxidase enzyme. Due to the observed link between heme content and catalytic activity, we suggest that the oxidase activity is catalyzed via the enzyme's heme center. RebD requires no exogenous cofactors for reaction, an unusual feature for an oxidase, given that the four-electron reduction of dioxygen to water calls for the provision of two additional electrons. Hence, the precise mechanistic strategy employed by RebD to catalyze the two-electron oxidative coupling of two molecules of IPA imine is still under investigation. Ongoing work using spectroscopic and crystallographic methods will be required to ascertain the exact mechanism that is involved.

Of particular interest is the fact that RebD contains, in addition to its heme cofactor, 1 equivalent of non-heme iron. While it is known that this iron does not form part of an iron−sulfur cluster, the exact form of this metal center has yet to be determined. Given the unusual oxidative chemistry that is observed, it is possible that this additional iron plays a role in electron transfer. Alternatively, examples exist in the literature of non-heme iron performing an apparent structural role (*27*, *28*), and that possibility cannot be eliminated at this stage. Further investigations will be required to determine the exact nature and function of this iron center.

Regardless, it has been established that the two-electron oxidative condensation of two molecules of IPA imine is the favored in vitro pathway for RebD-mediated CPA formation. Condensation of an IPA imine with its corresponding enamine tautomer would yield **5**, a cross-conjugated imine that is four-electron-oxidized relative to the two L-Trp substrates of RebO (Scheme 2). We favor this intermediate as a substrate for the oxidative coupling step due both to the inherent stability of its highly conjugated skeleton and to its ability to participate in one-electron oxidation steps

Scheme 2: Proposed Mechanism for CPA Formation, Involving Initial Formation of the Dimerized Conjugated Imine (**5**) and Subsequent Two-Electron Oxidation To Give CPA (**4**)

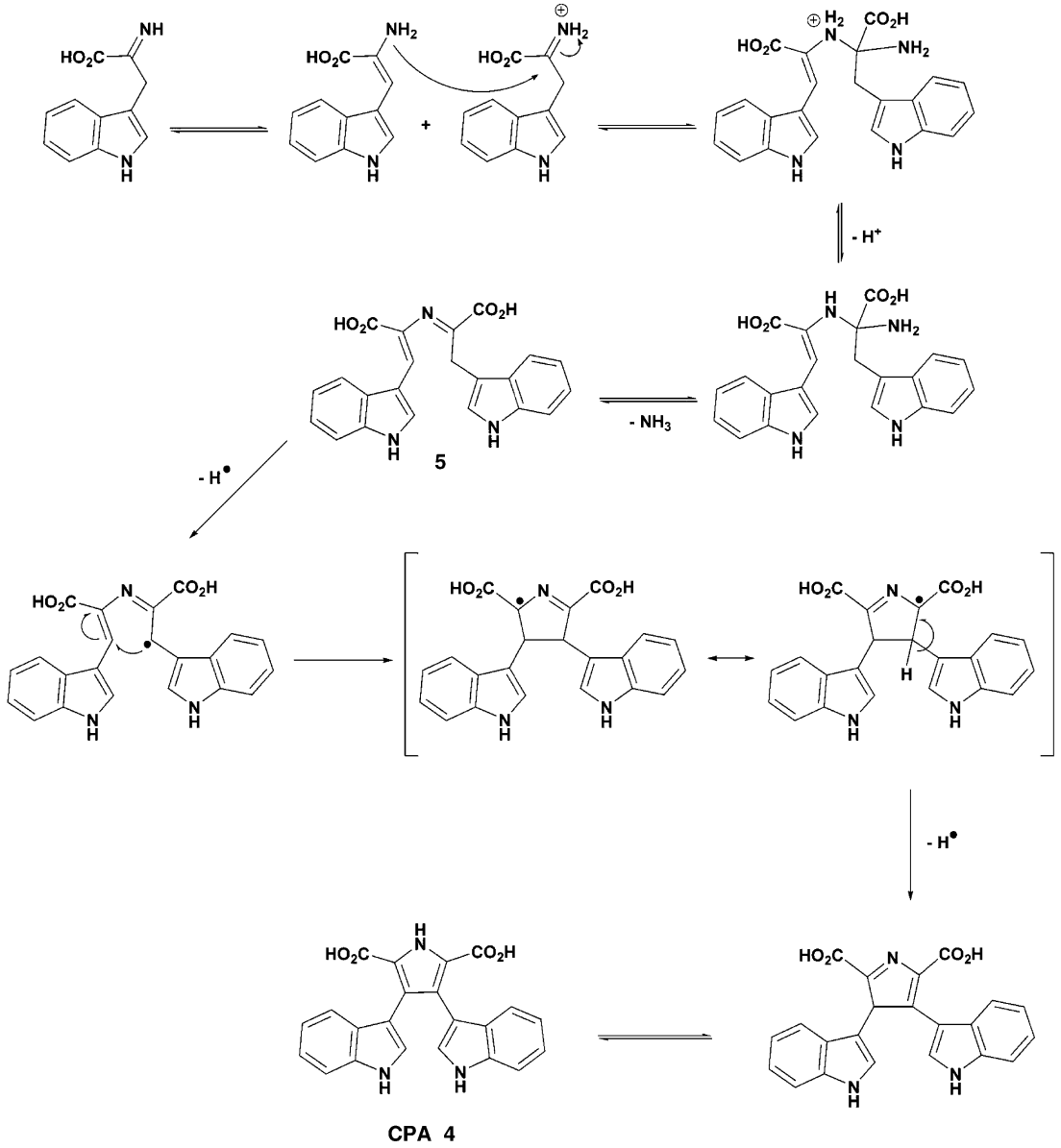

involving hydrogen abstraction, for example, from a single carbon center. This obviates the need for conformational or orientational changes during catalysis. The net two-electron oxidation by RebD to give CPA may occur in one-electron steps as shown (Scheme 2). This would furnish the dicarboxypyrrole **4** through formation of the pyrrolic C_3-C_4 bond, followed by tautomerization. The role of the heme (and/or non-heme) iron center in the passage of substrate-derived electrons to dioxygen, and the detection of any substrate-based radicals, will be the subject of future study on the RebO/RebD system.

In reconstituting the biosynthetic pathway to CPA (**4**), via heterologous expression of RebO and RebD, we have demonstrated the overall biosynthetic route to this key rebeccamycin pathway intermediate. The preference of these two enzymes to operate in tandem is an elegant example of the ability of Nature to shield and channel reactive intermediates through complex biosynthetic transformations. The overall six-electron oxidation of the two L-Trp substrates to yield CPA represents very interesting oxidation chemistry. The apparent two-electron oxidative coupling involved in RebD-mediated turnover is of particular interest. This study thus forms a platform for mechanistic investigations into the unusual oxidase activity observed for the hemoprotein, RebD.

ACKNOWLEDGMENT

We thank Prof. Robert S. Phillips for providing an authentic sample of 7Cl-Trp. We thank Ellen Yeh for assistance with preliminary experiments and Ellen Yeh and Frédéric H. Vaillancourt for helpful discussions.

REFERENCES

1. Moreau, P., Anizon, F., Sancelme, M., Prudhomme, M., Bailly, C., Severe, D., Riou, J.-F., Fabbro, D., Meyer, T., and Aubertin, A.-M. (1999) Syntheses and biological activities of rebeccamycin analogues. Introduction of a halogenoacetyl substituent, *J. Med. Chem. 42*, 584−592.
2. Tamaoki, T., Nomoto, H., Takahashi, I., Kato, Y., Morimoto, M., and Tomita, F. (1986) Staurosporine, a potent inhibitor of phospholipid/Ca^{2+} dependent protein kinase, *Biochem. Biophys. Res. Commun. 135*, 397−402.

3. Saif, M. W., and Diasio, R. B. (2005) Edotecarin: A novel topoisomerase I inhibitor, *Clin. Colorectal Cancer 5*, 27−36.
4. Senderowicz, A. M. (2003) Novel small molecule cyclin-dependent kinases modulators in human clinical trials, *Cancer Biol. Ther. 2*, S84−S95.
5. Hussain, M., Vaishampayan, U., Heilbrun, L. K., Jain, V., LoRusso, P. M., Ivy, P., and Flaherty, L. (2003) A phase II study of rebeccamycin analog (NSC-655649) in metastatic renal cell cancer, *Invest. New Drugs 21*, 465−471.
6. Facompre, M., Goossens, J.-F., and Bailly, C. (2001) Apoptotic response of HL-60 human leukemia cells to the antitumor drug NB-506, a glycosylated indolocarbazole inhibitor of topoisomerase 1, *Biochem. Pharmacol. 61*, 299−310.
7. Sánchez, C., Butovich, I. A., Braña, A. F., Rohr, J., Méndez, C., and Salas, J. A. (2002) The biosynthetic gene cluster for the antitumor rebeccamycin: Characterization and generation of indolocarbazole derivatives, *Chem. Biol. 9*, 519−531.
8. Sánchez, C., Zhu, L., Braña, A. F., Salas, A. P., Rohr, J., Méndez, C., and Salas, J. A. (2005) Combinatorial biosynthesis of antitumor indolocarbazole compounds, *Proc. Natl. Acad. Sci. U.S.A. 102*, 461−466.
9. Onaka, H., Taniguchi, S.-I., Igarashi, Y., and Furumai, T. (2002) Cloning of the staurosporine biosynthetic gene cluster from *Streptomyces* sp. TP-A0274 and its heterologous expression in *Streptomyces lividans*, *J. Antibiot. 55*, 1063−1071.
10. Onaka, H., Taniguchi, S.-I., Igarashi, Y., and Furumai, T. (2003) Characterization of the biosynthetic gene cluster of rebeccamycin from *Lechevalieria aerocolonigenes* ATCC 39243, *Biosci., Biotechnol., Biochem. 67*, 127−138.
11. Salas, A. P., Zhu, L., Sánchez, C., Braña, A. F., Rohr, J., Méndez, C., and Salas, J. A. (2005) Deciphering the late steps in the biosynthesis of the anti-tumour indolocarbazole staurosporine: Sugar donor substrate flexibility of the StaG glycosyltransferase, *Mol. Microbiol. 58*, 17−27.
12. Onaka, H., Asamizu, S., Igarashi, Y., Yoshida, R., and Furumai, T. (2005) Cytochrome P450 homolog is responsible for C−N bond formation between aglycone and deoxysugar in the staurosporine biosynthesis of *Streptomyces* sp. TP-A0274, *Biosci., Biotechnol., Biochem. 69*, 1753−1759.
13. Yeh, E., Garneau, S., and Walsh, C. T. (2005) Robust in vitro activity of RebF and RebH, a two-component reductase/halogenase, generating 7-chlorotryptophan during rebeccamycin biosynthesis, *Proc. Natl. Acad. Sci. U.S.A. 102*, 3960−3965.
14. Nishizawa, Y., Aldrich, C. C., and Sherman, D. H. (2005) Molecular analysis of the rebeccamycin L-amino acid oxidase from *Lechevalieria aerocolonigenes* ATCC 39243, *J. Bacteriol. 187*, 2084−2092.
15. Sambrook, J., and Russell, D. W. (2000) *Molecular cloning: A laboratory manual*, 3rd ed., Cold Spring Harbor Laboratory Press, Plainview, NY.
16. Bradford, M. M. (1976) A rapid and sensitive method for the quantitation of microgram quantities of protein utilizing the principle of protein-dye binding, *Anal. Biochem. 72*, 248−254.
17. Berry, E. A., and Trumpower, B. L. (1987) Simultaneous determination of hemes *a*, *b*, and *c* from pyridine hemochrome spectra, *Anal. Biochem. 161*, 1−15.
18. Heigler, B. E., and Gibson, D. T. (1990) Purification and properties of NADH-ferredoxinNAP reductase, a component of naphthalene dioxygenase from *Pseudomonas* sp. strain NCIB 9816, *J. Bacteriol. 172*, 457−464.
19. Fröde, F., Hinze, C., Josten, I., Schmidt, B., Steffan, B., and Steglich, W. (1994) Isolation and synthesis of 3,4-bis(indol-3-yl)pyrrole-2,5-dicarboxylic acid derivatives from the slime mould *Lycogala epidendrum*, *Tetrahedron Lett. 35*, 1689−1690.
20. Delieu, T., and Walker, D. A. (1972) An improved cathode for the measurement of photosynthetic oxygen evolution by isolated chloroplasts, *New Phytol. 71*, 201−225.
21. Vaillancourt, F. H., Han, S., Fortin, P. D., Bolin, J. T., and Eltis, L. D. (1998) Molecular basis for the stabilization and inhibition of 2,3-dihydroxybiphenyl 1,2-dioxygenase by *tert*-butyl alcohol, *J. Biol. Chem. 273*, 34887−34895.
22. Ueda, M., Chang, C.-C., and Ohno, M. (1988) Purification and characterization of L-amino acid oxidase from the venom of *Trimeresurus mucrosquamatus* (Taiwan habu snake), *Toxicon 26*, 695−706.
23. Lovenberg, W., Buchanan, B. B., and Rabinowitz, J. C. (1963) Studies on the chemical nature of clostridial ferredoxin, *J. Biol. Chem. 238*, 3899−3913.
24. Chen, J.-S., and Mortenson, L. E. (1977) Inhibition of methylene blue formation during determination of the acid-labile sulfide of iron−sulfur protein samples containing dithionite, *Anal. Biochem. 79*, 157−165.
25. August, P. R., Grossman, T. H., Minor, C., Draper, M. P., MacNeil, I. A., Pemberton, J. M., Call, K. M., Holt, D., and Osburne, M. S. (2000) Sequence analysis and functional characterization of the violacein biosynthetic pathway from *Chromobacterium violaceum*, *J. Mol. Microbiol. Biotechnol. 2*, 513−519.
26. Ruhul Momen, A. Z. M., and Hoshino, T. (2000) Biosynthesis of violacein: Intact incorporation of tryptophan molecule on the oxindole side, with intramolecular rearrangement of the indole ring on the 5-hydroxyindole side, *Biosci., Biotechnol., Biochem. 64*, 539−549.
27. Colabroy, K. L., Zhai, H., Li, T., Ge, Y., Zhang, Y., Liu, A., Ealick, S. E., McLafferty, F. W., and Begley, T. P. (2005) The mechanism of inactivation of 3-hydroxyanthranilate-3,4-dioxygenase by 4-chloro-3-hydroxyanthranilate, *Biochemistry 44*, 7623−7631.
28. Zhang, Y., Colabroy, K. L., Begley, T. P., and Ealick, S. E. (2005) Structural studies on 3-hydroxyanthranilate-3,4-dioxygenase: The catalytic mechanism of a complex oxidation involved in NAD biosynthesis, *Biochemistry 44*, 7632−7643.

BI051706E